Effect of layer orientation and infill density on reliability and lifetime of FDM-printed conductive composites under tensile loading

Nassima Naboulsi, Fouad Ait Hmazi, Fatima Majid
Laboratory of Nuclear, Atomic, Molecular, Mechanical and Energetic Physics, Chouaib Doukkali University, El Jadida, Morocco
naboulsi.n@ucd.ac.ma, https://orcid.org/0009-0003-3493-2519

Fatima Zahra Karmil
Laboratory of Physical Chemistry of Materials, Department of Chemistry, Faculty of Sciences, University Chouaïb Doukkali, P.O.Box 20, El Jadida 24000, Morocco.

Narjisse Douiri
Electrical Engineering and Intelligent Systems Laboratory (EEIS), ENSET Mohammedia, Hassan II University of Casablanca, Morocco

Taoufik Hachimi
Ecole Normale Supérieure (ENS), Moulay Ismaïl University, BP. 3104, Toulal, Meknes, Morocco
Laboratory of Nuclear, Atomic, Molecular, Mechanical and Energetic Physics, University Chouaib Doukkali, El Jadida, Morocco

ABSTRACT. Conductive composites have attracted growing interest in recent years in the field of additive manufacturing, especially for functional and structural applications. Nevertheless, their mechanical behavior and durability remain highly influenced by 3D printing methods and parameters. This paper investigates the combined effect of layer orientation and infill density on the mechanical damage and reliability of PLA-CB conductive composites manufactured by filament deposition modeling (FDM) technology. Tensile tests were performed on specimens printed with different layer orientations (0°, 45° and 90°) and infill densities (20%, 40%, 60%, 80% and 100%) to analyze the evolution of damage and the dispersion of mechanical properties. Analysis of damage evolution was used to model failure probability, assess material reliability, and predict service life based on 3D printing parameters. The results indicate that infill density significantly influences mechanical strength and performance stability, while layer orientation also plays a key role in the failure mechanism. The 0° orientation (parallel to the tensile direction)

Citation: Naboulsi, N., Karmil F.Z., Douiri, N., Ait Hmazi, F., Hachimi, T., Majid, F., Effect of layer orientation and infill density on reliability and lifetime of FDM-printed conductive composites under tensile loading, Fracture and Structural Integrity, 78 (2026) 74-95.

Received: 23.05.2026
Accepted: 22.07.2026
Published: 25.07.2026
Issue: 10.2026

offered the best mechanical performance. At 45°, the results show intermediate behavior between stiffness and flexibility due to the distribution of shear stresses between layers. However, samples printed at 90° show much lower strength, dominated by delamination between layers. This study thus proposes a useful predictive framework for optimizing the printing parameters of PLA-CB conductive composites and contributes to a better understanding of their behavior in service for applications requiring reliable and durable mechanical performance.

KEYWORDS. Conductive composites, Fused deposition modeling, Tensile tests, Layer orientation, Infill density, Reliability, Damage.

INTRODUCTION

Researchers have become increasingly interested in alternative methods for predicting the service life of components manufactured using fused deposition modeling (FDM) technology through design approaches that prevent fatigue failure, with the aim of improving the reliability and durability of 3D-printed structures throughout their lifecycle [1,2]. Among the available approaches, the two-parameter Weibull statistical model has become one of the most widely used techniques for assessing the variability of mechanical strength and estimating the reliability of polymer-based materials under various experimental conditions [3,4]. Additive manufacturing (using FDM), is based on the superposition of successive layers, which inevitably leads to variations in the mechanical properties of printed parts. Most of these variations can be explained by the quality of the interlayer bond, the alignment of the filaments, and the porosity that may remain within the part.

However, the mechanical behavior of FDM-printed components is not governed only by the nominal parameters defined in the slicing software. After printing, the actual geometry of the part may differ from the designed model due to process-induced deviations such as local voids, bead discontinuities, dimensional inaccuracies, incomplete filament deposition, imperfect interlayer bonding, and defect formation during material extrusion. In this regard, D'Andrea et al. demonstrated that failure analysis is essential for establishing a correlation between the mechanical behavior and microstructural characteristics of materials, using infrared thermography to identify the "limit stress level" that triggers the first irreversible damage within the printed structure [5]. Meanwhile, the work of Tabatabaee and Fakoor highlights that porosity and the presence of irregularly shaped cavities which are inherent to the FDM process systematically reduce the modulus of elasticity and ultimate stress, necessitating the use of reinforced isotropic solid models to describe the material's effective properties [6]. The study by Hachimi et al. reinforces this analysis by demonstrating that the mechanical properties of PLA degrade in proportion to the size of defects and artificial cracks, and that a probabilistic approach can be used to define the reliability of a part based on the critical crack length[7]. In an other research, he highlight a fundamental geometric deviation: the actual cross-section of the deposited filaments is not circular but oval-rectangular due to flattening during extrusion; ignoring this physical reality can lead to prediction errors exceeding 15% in stress simulations, making it essential to calibrate a "virtual raster cross-section" to ensure the accuracy of numerical models [8].These post-printing non-uniformities can strongly affect stress transfer, crack initiation, and failure propagation, and therefore must be considered when interpreting tensile properties and reliability indicators. In order to better anticipate these variations, Weibull statistical analysis has proven particularly useful: it allows us to estimate the probability that a component may survive or break, and to evaluate its actual service life in response to mechanical stress [9,10].

As part of this study, we applied Weibull analysis to tension test data in order to study the behavior of critical stress, strain, and failure time under different FDM printing configurations. In particular, we tested samples printed with three layer orientations (0°, 45°, and 90°) and five infill densities ranging from 20% to 100%. This aspect is particularly important for low infill densities, where the real printed morphology may be more sensitive to large internal gaps, discontinuous load-bearing paths, bead irregularities, and local defects generated during deposition. In such cases, the nominal infill percentage alone may not fully describe the effective load-bearing structure, which can lead to higher dispersion in tensile properties and reliability metrics. This statistical approach provided a better understanding of how these manufacturing parameters influence the material's long-term reliability and expected service life [11–13].

In this regard, some authors emphasize that advanced characterization of internal voids is essential, as these defects; which are often oriented along the printing direction; create geometric deviations whose dispersion (such as segment waviness) can be modeled by a Weibull distribution[14,15]. Other studies specify that low fill densities create a mesostructure of air cavities that act as crack propagators under stress, making mechanical strength inseparable from the management of these internal voids [15,16]. Finally, the study by Parodo et al. on ABS highlights the critical limitations of the FDM process for ultra-low densities (5%), where dimensional instability and increased structural brittleness are observed, in contrast to higher densities, which ensure better geometric fidelity and superior structural integrity [17]. This study explores potential improvements to the performance of a 3D-printed conductive composite based on polylactic acid incorporating with 40% of carbon black (PLA-CB) [18,19]. This composite retains the ease of fabrication and biodegradability of conventional PLA while improving electrical conductivity through the addition of carbon black particles [20,21]. However, conductive fillers can also alter the material's mechanical properties by modifying its internal structure and interfacial interactions [22]. This was also examined in this study by comparing PLA-CB with pure PLA on multiple instances.

In this regard, the goal of the current study is to investigate how fill density and layer orientation affect the tensile mechanical performance of PLA-CB composites made by FDM. Samples printed with various layer orientations and fill densities were subjected to tensile testing in order to assess the resulting differences in mechanical properties and obtain a better understanding of the related failure mechanisms. Particular attention was given to the effect of these printing parameters on interlayer adhesion, internal void formation, stress transfer within the structure, and crack initiation and propagation during tensile loading. By considering both nominal slicing parameters and possible post-printing defects, this work aims to provide a more realistic interpretation of the mechanical reliability of PLA-CB printed specimens under tensile loading.

MATERIALS AND METHODS

3D Printing Process

Additive manufacturing, is a 3D printing process used to build a physical product layer by layer from a digital file (3D CAD model) [23,24]. This technology is based on a key five-step process. Initially, a 3D model must be designed on a computer (CAD). Secondly, the 3D model is converted into an STL file, which is the most commonly used format for 3D printing. The STL file is then uploaded to slicing software designed for 3D printing. In the next step, this software slices the model layer by layer and defines the print path for each layer. These instructions are saved as a G-code, a language for computerized machine tools that summarizes all the motor instructions (path to follow, speed of movement, motors required, etc.). After the code is sent to the 3D printer machine, 3D printing begins by building the desired part layer by layer. This process allows for the design of personalized and innovative parts. Among the best-known 3D printing methods are stereolithography (SLA), selective laser sintering (SLS), material projection, and fused deposition modeling (FDM), also known as fused filament fabrication (FFF) [25,26]. The latter is the most common technology for polymers; it is based on the extrusion of a heated filament that is deposited in layers. FDM/FFF will be the method used in this paper because of its simplicity, low cost, and wide accessibility.

Fused filament fabrication (FFF) process

Fused filament fabrication (FFF/FDM) is one of the most widespread and commonly used 3D printing techniques due to its simplicity, low cost, and accessibility. The process begins by adding a spool of thermoplastic conductive filament (PLA-CB) to the printer [27]. Using an extrusion motor, the filament is continuously pushed toward a small heating chamber located in the print head. The filament is then heated to its melting point and pushed out of the nozzle, then deposited layer by layer on a printing bed following the trajectory defined by the G-code file, generated from the initially designed 3D model. Each layer cools and solidifies quickly until the final part is obtained [28], see Fig. 1.

Influence of printing and slicing parameters

Several factors may influence the quality of the final 3D printed part during the printing process. As shown in the Ishikawa diagram in Fig. 2, temperature parameters such as (nozzle, build plate, enclosure, and cooling) affect the level of crystallinity of the polymer and therefore the melting of the filament and the adhesion between layers, leading to varied and complex thermal conditions and influencing the mechanical and electrical properties of the conductive composites. Printing speed is a determining factor in surface quality and geometric accuracy. Orientation is another key factor that directly affects mechanical strength and dimensional accuracy along the X, Y, and Z axes. The uniformity of the deposit can also be affected by environmental factors such as dust concentration, humidity, and ambient temperature. Furthermore, the strength of the printed part depends on infill parameters such as density, pattern, orientation, and speed. Finally, material factors associated with the condition and calibration of the device (mechanical stability, build plate quality, nozzle diameter, extrusion system

[29,30] have a significant impact on process reliability. The optimization of all these elements leads to a high-quality final printed product [31].

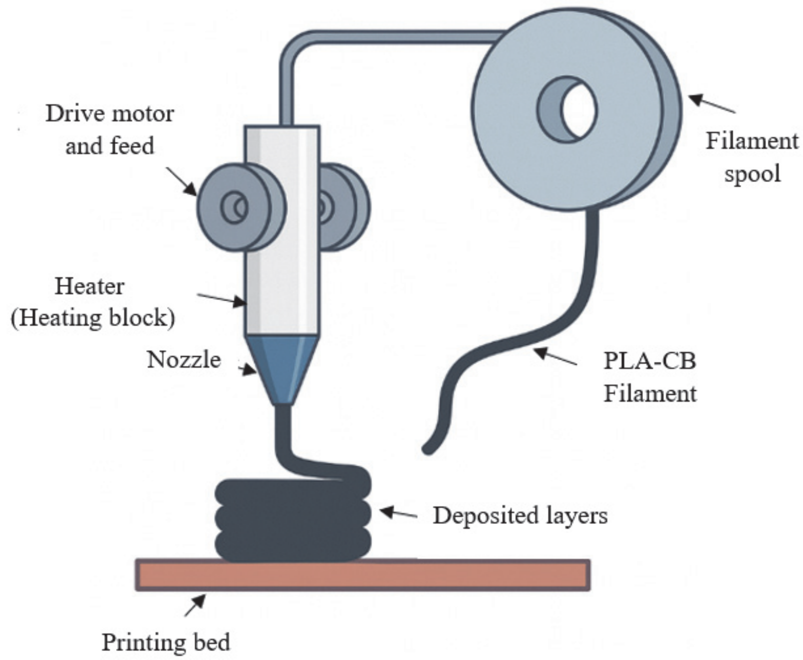

Figure 1: Graphical representation of the Fused Filament Fabrication (FFF) process.

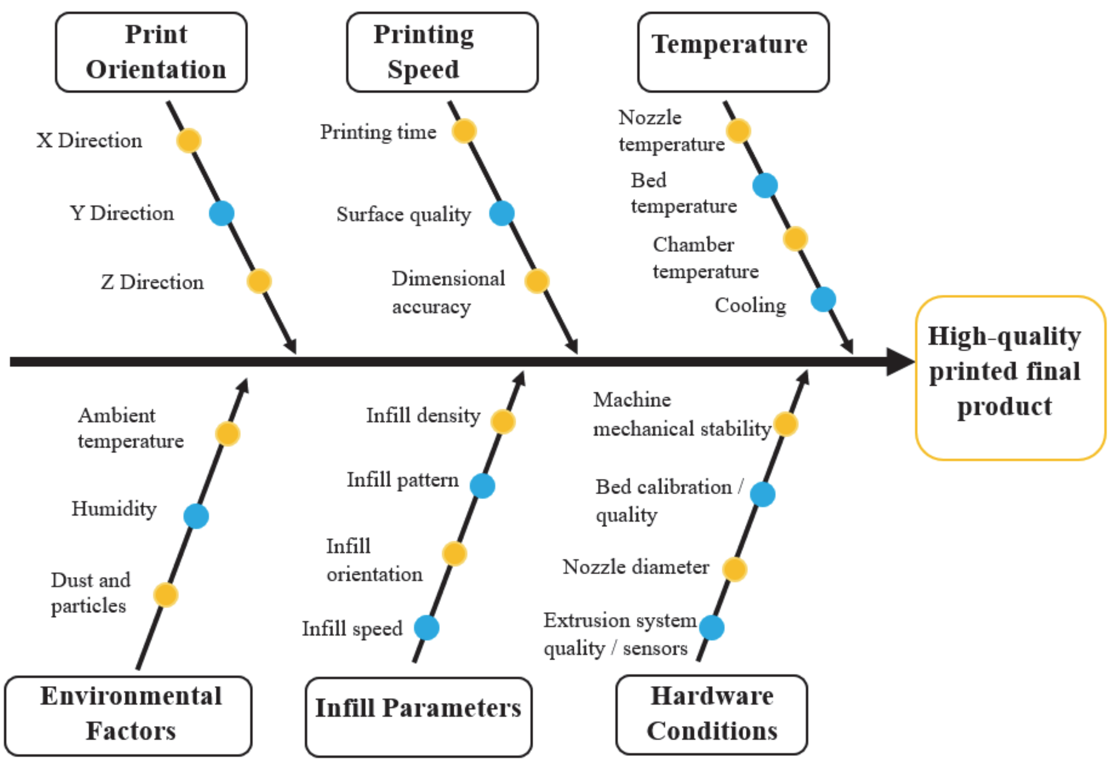

Figure 2: Ishikawa diagram showing factors influencing the quality of 3D printed parts.

Tensile tests

The mechanical tests were performed using an MTS Criterion Model 43 universal testing machine with a maximum load capacity of 30 kN. Although the machine allows a crosshead speed range from 0.005 mm/min to 1,020 mm/min, the crosshead speed was fixed at 1 mm/min according to the standard for all specimens in this study. The machine was connected to a computer running MTS TestSuite software, which enabled real-time monitoring of the tensile tests through force-elongation curves.

In order to evaluate the influence of layers orientation and fill density on PLA-CB, three orientations were programmed: 0° (printed filaments parallel to the stress axis), 45° (cross-hatching), and 90° (filaments perpendicular to the stress axis). These orientations control anisotropy: at 0°, the load is mainly absorbed along the filaments; at 90°, the strength depends mainly on the adhesion between layers; and at 45°, the response combines opening and shearing at the interfaces. The fill density was adjusted to several levels (20%, 40%, 60%, 80%, and 100%) in order to modulate the internal porosity and the number of junctions between strands; a higher density increases the load-bearing section and cohesion, while a low density promotes the appearance and coalescence of voids, see Fig. 4. In order to isolate the effect of these two factors, all other printing parameters settings, such as extrusion temperature, layer height, and print speed, were kept constant based on the characteristics recommended by the filament supplier, see Tab. 1.

Parameter	Value
Printer model	FlashForge Creator 3 Pro
Slicing software	FlashPrint
Raster pattern	Linear
Number of perimeters/walls	3
Filament diameter	1.75 mm
Nozzle diameter	0.4 mm
Nozzle temperature (°C)	230
Layer height (mm)	0.2
Bed temperature (°C)	60
Printing speed (mm/s)	40

Table 1: FDM printing parameters used for PLA-CB specimen fabrication.

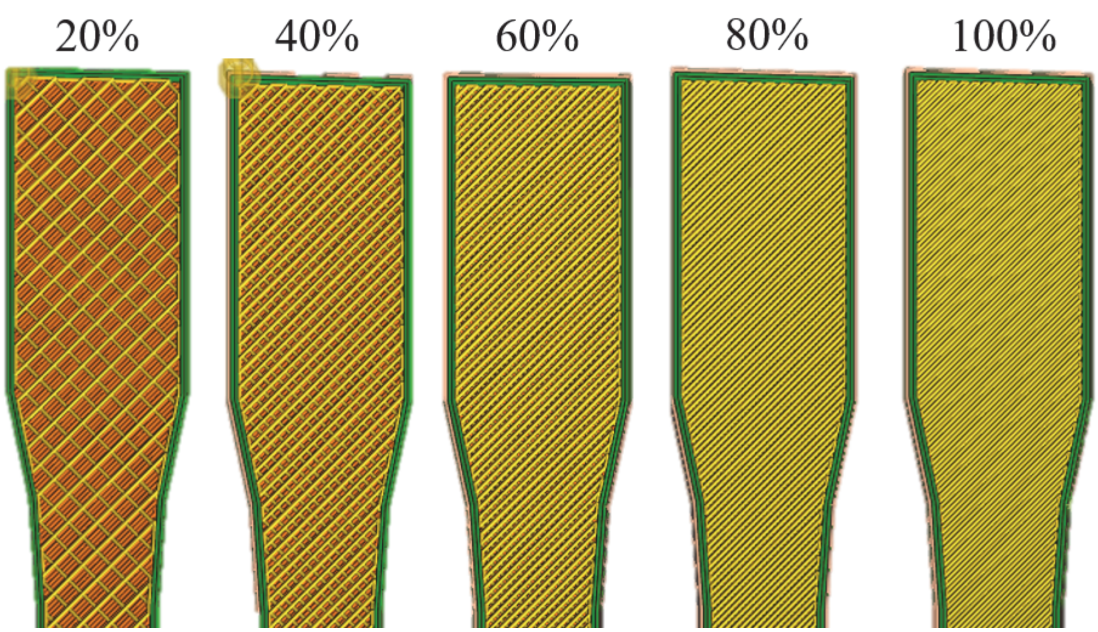

Figure 3: Slicer preview of the tensile specimen geometries showing the different infill density percentages investigated in this study.

The specimens were tested at room temperature. For each experimental configuration, five specimens were printed and tested in accordance with the ISO 527-2 Type 5A tensile testing standard, resulting in a total of 90 specimens, as shown in Tab. 2. This included 75 PLA-CB specimens (5 specimens × 5 infill densities × 3 printing orientations) and 15 pure PLA specimens (5 specimens × 3 printing orientations), which were used as reference samples at 100% infill density. This number of replicates was considered appropriate for comparing the mechanical response across the investigated printing conditions.

Fig. 4 shows tensile specimens printed at 90°, 45°, and 0°, with dimensions conforming to ISO 527-2 Type 5A. Fig. 5 presents tensile specimens printed at 90°, 45°, and 0° with different infill densities, before and after tensile testing, as well as an example of a specimen subjected to uniaxial tensile loading.

Material	Infill density	Printing Orientation	Number of specimens
PLA-CB	20%	0°	5
		45°	5
		90°	5
	40%	0°	5
		45°	5
		90°	5
	60%	0°	5
		45°	5
		90°	5
	80%	0°	5
		45°	5
		90°	5
	100%	0°	5
		45°	5
		90°	5
Pure PLA (As a reference)	100%	0°	5
		45°	5
		90°	5

Table 2: Experimental matrix of tensile tests performed on PLA-CB and pure PLA specimens.

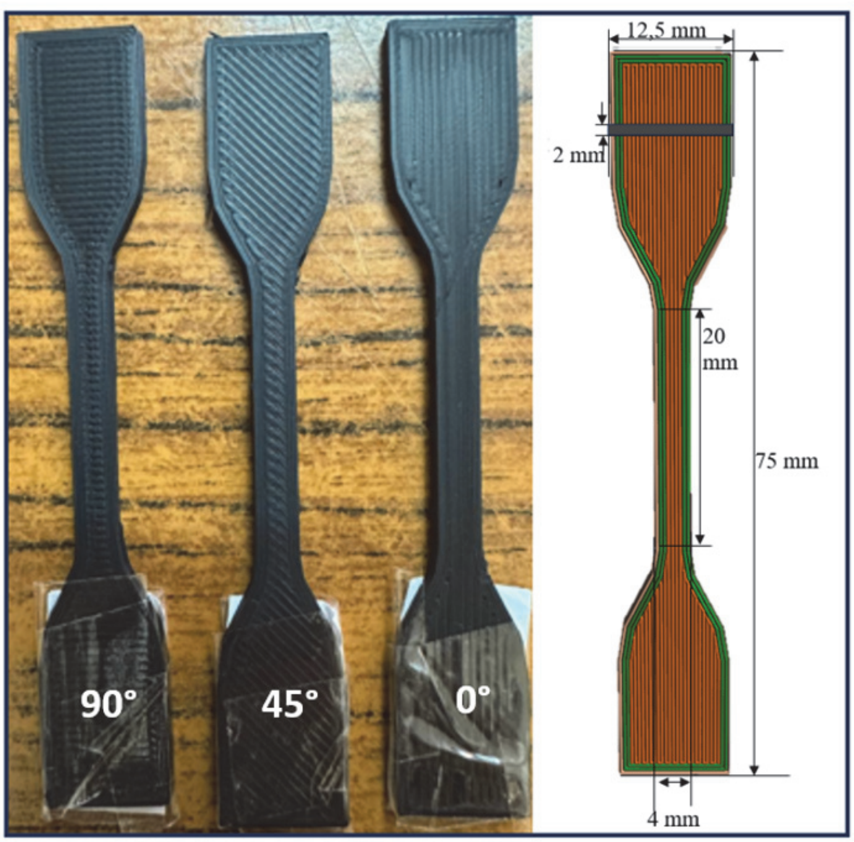

Figure 4: Tensile specimens printed at 90°, 45°, and 0°, with dimensions according to ISO 527-2 type 5A.

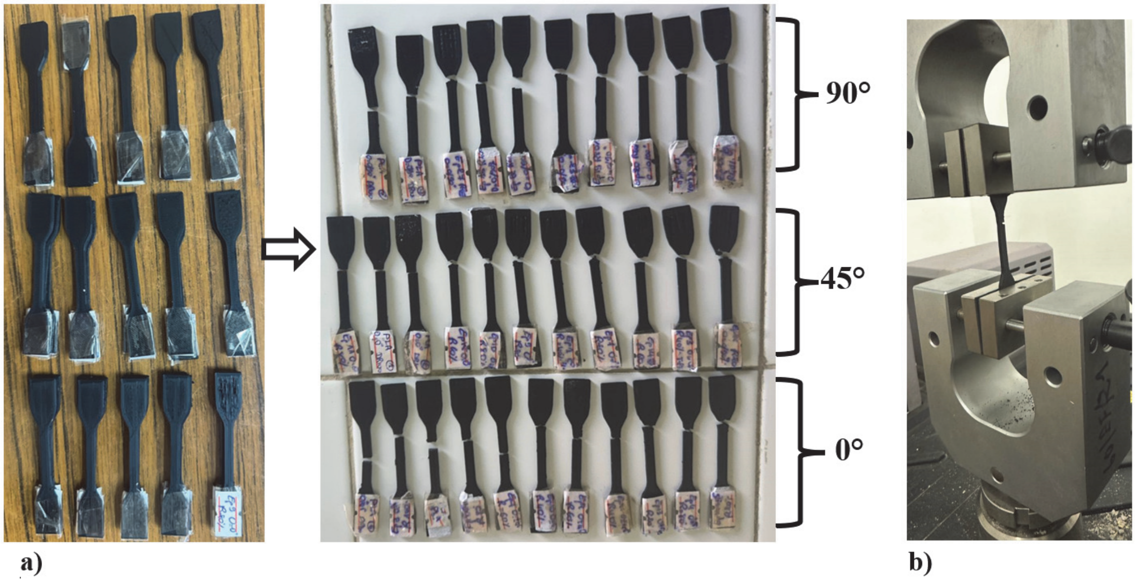

Figure 5: a) Tensile test specimens printed at 90°, 45°, and 0° orientations with different infill densities, before and after testing. b) Representative specimen under uniaxial loading.

Fig. 6 shows representative stress-strain curves obtained from tensile tests conducted on the PLA-CB composite and pure PLA (at 45° orientation and 100% infill density). Compared to PLA-CB, the curve for pure PLA exhibits higher maximum tensile stress value and a more pronounced initial slope, indicating greater intrinsic stiffness. The incorporation of carbon black into PLA appears to reduce both mechanical strength and may locally stiffen the polymer matrix, likely due to interfacial effects and the heterogeneous dispersion of conductive fillers that can compensate for this effect, leading to an overall apparent stiffness lower than pure PLA. These curves are presented for illustrative purposes to highlight typical mechanical characteristics.

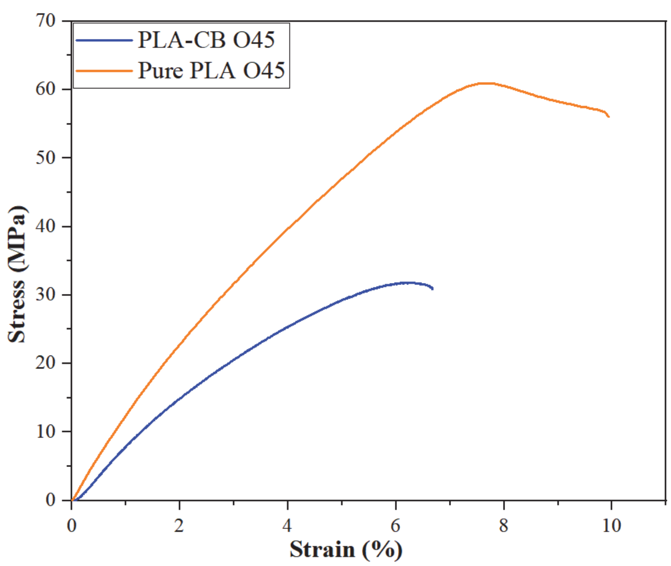

Figure 6: Representative tensile strength values of the PLA-CB composite and pure PLA printed at 45° orientation with 100% infill density.

Weibull analysis methodology

Weibull distribution model is one of the most widely used statistical methods for predicting the service life of materials under mechanical stresses. In this paper, the two-parameter Weibull; the shape parameter (m) and scale parameter (η); were determined using the linear regression approach. This method was selected because the analysis was based on a sseries of repeated tensile tests allowing a clear comparison of the tensile strength variability among the various printing orientations by obtaining the scale parameter from the intercept and the shape parameter from the slope of the fitted line. The comparison between orientations was supported by the combined interpretation of the Weibull parameters, the linear fitting quality, and the corresponding survival-failure probability curves, providing a consistent evaluation of strength dispersion and characteristic mechanical behavior. The model for linear regression is expressed as follows:

$$\mathrm{Ln}\left(\ln\left(\frac{1}{1-F(x;\mathrm{m},\eta)}\right)\right)=\mathrm{m}\ln(x)-\mathrm{m}\ln(\eta) \tag{1}$$

with F(x; m, η) represent the experimental ultimate stress and strain values ranked in ascending order, and the corresponding empirical failure probabilities were subsequently calculated for the Weibull analysis.

RESULTS AND DISCUSSION

Effect of infill densities

Tensile tests were performed on all printed samples prepared in compliance with ISO 527-2 Type 5A at different infill densities (20%, 40%, 60%, 80%, and 100%) and printing orientations (0°, 45°, and 90°). The data acquisition system connected to the tensile testing machine recorded the force measured by the force sensor and the displacement captured by the extensometers until the samples failure. Strain-stress curves (%- MPa) were generated for all samples from this raw data. These curves were then used to extract the relevant mechanical properties in order to analyze the influence of PLA-CB infill density at each print orientation [32]. This analysis is particularly important for low infill densities, where the printed structure contains larger internal gaps and fewer continuous load-bearing paths, which may increase the sensitivity of the specimens to local printing non-uniformities and contribute to the dispersion of the tensile results.

For Orientation 0°:

Fig. 7 shows the stress-strain curves reflecting the tensile behavior of PLA-CB and pure PLA for a layer orientation of 0°. The mechanical characteristics derived from these curves are shown in Tab. 3. The pure PLA with 100% filling density has the highest maximum stress, reaching 58.181 MPa, with an elongation at break of 14.332%, reflecting good stiffness combined with a certain degree of ductility.

The comparison with the curves for the PLA-CB confirms that the composites present a lower mechanical performance overall, confirming the brittle effect of CB within the PLA matrix. However, the infilling density also has a significant effect on the results: for low densities between 20% and 40%, the maximum stress is limited to 25.306 and 26.163 MPa respectively, with early failure at approximately 4.474 to 4.740% deformation. This decrease can be explained by the presence of internal voids which decrease the effective surface for the stress transmission and promote the initiation of cracks. The tensile strength slightly increased from 28.582 to 29.608 MPa with the increase of density from 60 to 80% and the elongation was about 5.052 to 5.432%. The increase in material content therefore improves the compactness of the structure and interlayer cohesion, which slightly delays failure. However, the embrittlement induced by CB remains apparent.

Finally, at 100% density, PLA-CB shows a clear improvement, with a maximum stress of 49.680 MPa and an elongation of approximately 6.555%. Although this value is still lower than the value for pure PLA, it demonstrates the positive effect of a fully dense structure, which reduces internal defects and allows for better load transmission along the tensile axis. We note that the increase in filling density partially offsets the loss in mechanical performance caused by the conductive filler. This confirms that filling density is a key parameter for optimizing the mechanical properties of printed parts. Although pure PLA still exhibits higher strength and ductility, fully dense PLA-CB represents an interesting compromise, combining relatively high mechanical strength with the functional potential associated with conductivity.

For Orientation 90°:

Fig. 8 presents the effect of infill density on the tensile properties of PLA-CB samples with a layer orientation of 90°. Maximum stresses are generally much lower than at 0°, which is a proof of the vulnerability of parts with filaments oriented perpendicularly to the tensile axis. The ultimate stress is still limited to about 23.481 to 24.415 MPa with early failure at about 5.626 to 5.727% strain at low densities of 20 to 40%. These values indicate a high fragility due to the larger internal voids and the stress pattern that is adverse to interlayer bonding. With increase in density from 60 to 80%, there is a slight increase in strength to 25.650 to 32.671 MPa for elongation of around 5.931 to 6.706%. This shows the improvement in internal cohesion.

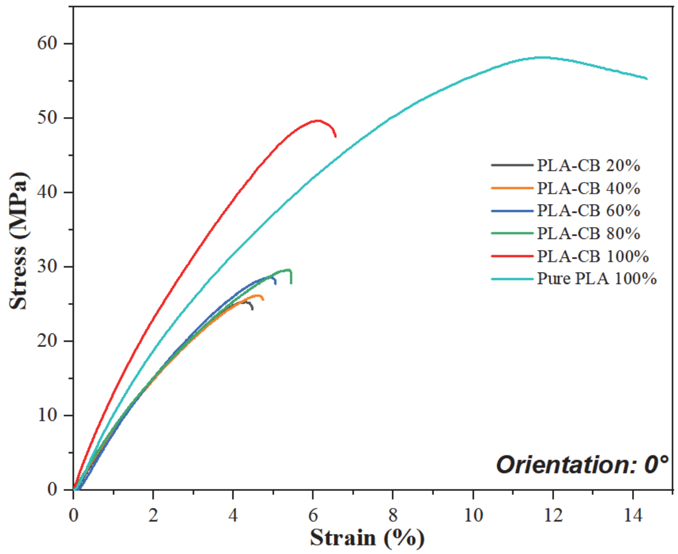

Figure 7: Stress-strain curves showing the effect of infill density on 3D-printed PLA-CB specimens at 0° orientation.

Infill density (%) for 0° orientation	PLA-CB					Pure PLA
	20%	40%	60%	80%	100%	100%
Maximum stress (MPa)	25.306	26.163	28.582	29.608	49.680	58.181
Fracture stress (MPa)	24.286	25.582	27.745	29.278	47.530	55.323
Elongation at break (%)	4.474	4.740	5.052	5.432	6.555	14.332

Table 3: Mechanical properties of PLA-CB at different infill densities for a 0° layer orientation.

PLA-CB at 100% exhibits a more robust behaviour with a maximum stress close to 32.671 MPa which is still smaller than the value obtained at 0° for the same density. This difference can be ascribed to the decisive contribution of filament orientation in force transmission. In contrast, pure PLA has a clear superiority with max stress 56.960 MPa, elongation more than 9.4%, which confirms the embrittlement due to the incorporation of carbon black. The mechanical properties for each infilling density at 90° orientation are shown in Tab. 3.

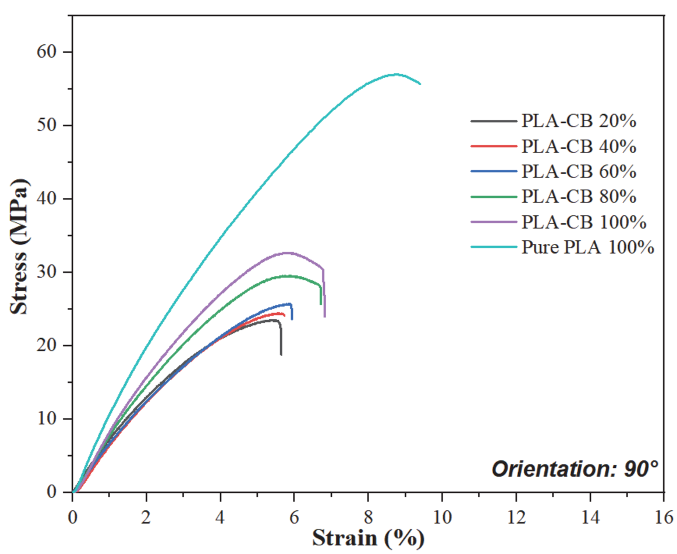

Figure 8: Stress-strain curves showing the effect of infill density on 3D-printed PLA-CB specimens at 90° orientation.

Infill density (%) for 90° orientation	PLA-CB					Pure PLA
	20%	40%	60%	80%	100%	100%
Maximum stress (MPa)	23.481	24.415	25.650	29.494	32.671	56.960
Fracture stress (MPa)	22.116	24.103	23.595	27.561	23.960	55.648
Elongation at break (%)	5.626	5.727	5.931	6.706	6.819	9.4

Table 4: Mechanical properties of PLA-CB at different infill densities for a 90° layer orientation.

For Orientation 45°:

For the 45° printing orientation, the stress-strain curves in Fig. 9 indicate an intermediate mechanical response between the two extreme orientations (0° and 90°). The maximum tensile stress is limited at low infill densities between 20 and 40% (19.093 - 23.787 MPa), with failure occurring at strains between 4.086 and 5.872%. This can be explained by the presence of large internal voids and the arrangement of the filaments in an inclined manner that decreases the effectiveness of the load transfer inside the structure. The failure of the specimens is by a combined mechanism of crack opening and shear deformation, which is evident in the SEM micrographs in Fig. 12. Some improvement of tensile performance can be found when the infill density increases from 60% to 80%. The ultimate stress is increased to between about 24.643 MPa and 25.645 MPa, and the elongation at break ranges from 6.047% and 6.499%. This trend suggests a gradual increase in internal cohesion with decreasing void fraction in the printed structure. However, the mechanical performance is still limited by the inclined filament layout corresponding to the 45° orientation. Under tensile loading part of the applied stress is transformed into shear stresses at the interlayer interfaces which reduces the total load bearing capacity of the material.

At 100% infill density, the PLA-CB specimens exhibit their highest mechanical performance for this orientation, reaching a maximum stress of about 31.811 MPa with an elongation at break close to 6.673%. Despite this improvement, these values remain considerably lower than those measured for pure PLA, which reaches nearly 60.944 MPa with an elongation of 9.933%, as shown in Tab. 5. This difference highlights the weakening effect associated with the incorporation of carbon black and confirms the strong influence of printing orientation on the mechanical behavior of the printed structures.

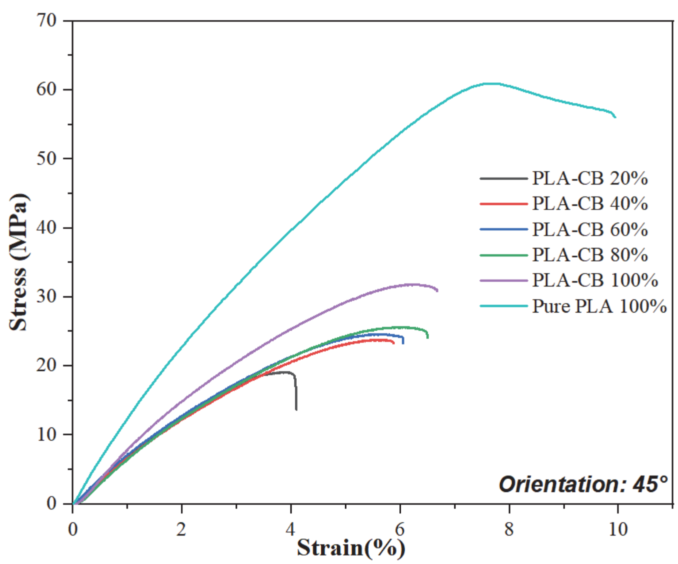

Figure 9: Stress-strain curves showing the effect of infill density on 3D-printed PLA-CB specimens at 45° orientation.

Infill density (%) for 45° orientation	PLA-CB					Pure PLA
	20%	40%	60%	80%	100%	100%
Maximum stress (MPa)	19.093	23.787	24.643	25.645	31.811	60.944
Fracture stress (MPa)	16.752	23.280	23.288	24.107	30.842	56.049
Elongation at break (%)	4.086	5.872	6.047	6.499	6.673	9.933

Table 5: Mechanical properties of PLA-CB at different infill densities for a 45° layer orientation.

Effect of Layer Orientation at 100% Infill Density

The curves in Fig. 10 clearly highlight the combined effect of layer orientation and the addition of carbon black on tensile mechanical properties. For pure PLA, the 45° orientation provides the highest strength, with a maximum stress of approximately 60.944 MPa and an elongation above 9.933 %. The 0° orientation ranks second, with a slightly lower ultimate stress of approximately 58.181 MPa, but it retains a higher elongation of 14.332 % due to the alignment of the filaments with the tensile axis, which promotes a homogeneous transfer of stresses and allows for more gradual deformation before rupture. For the 90° orientation, the maximum tensile strength is at its lowest level at around 56.960 MPa, but it maintains a higher elongation than the 45° orientation thanks to interlayer slippage.
Meanwhile, PLA-CB shows a clear drop in performance, no matter the orientation angle, compared to pure PLA. At 0°, the max stress hits about 49.680 MPa, but the elongation is limited to 6.555%. At orientations of 45° and 90°, the values decrease considerably, with strengths close to 32.662 and 31.798 MPa and limited elongation of 6.819 and 6.673%, respectively. The PLA-CB specimens printed at 45° and 90° show comparable tensile strength values under the measured conditions, as seen by the comparatively small variation of 0.86 MPa between them. These results confirm the weakening effect of carbon black, which causes cracks to form within the filaments and reduces interlayer adhesion, leading to premature breakage. Tab. 6 shows the mechanical properties of PLA-CB compared to PLA for each orientation.
As a result, the highest tensile strength for pure PLA was found at 45°, while the highest tensile strength for PLA-CB was found at 0°. Nonetheless, the strength values of the 45° and 90° PLA-CB specimens showed very close strength values. Overall, our findings imply that whereas off-axis orientations result in a more noticeable loss of mechanical performance, aligning the filaments parallel to the tensile axis enhances the tensile performance of PLA-CB and partially compensates the embrittling effect of carbon black.

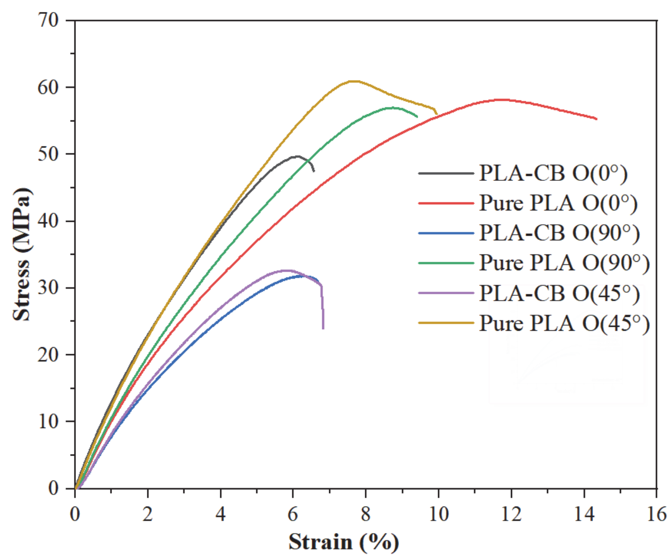

Figure 10: Stress-strain curves illustrating the effect of printing orientation on PLA-CB specimens with 100% infill density.

Orientations	PLA-CB			Pure PLA		
	Orientation 0°	Orientation 45°	Orientation 90°	Orientation 0°	Orientation 45°	Orientation 90°
Maximum stress (MPa)	49.680	32.662	31.798	58.181	60.944	56.960
Fracture stress (MPa)	47.530	23.961	30.842	55.323	56.049	55.648
Elongation at break (%)	6.555	6.819	6.673	14.332	9.933	9.4

Table 6: Mechanical properties of PLA-CB tensile test specimens with different orientations at 100% infill density.

SEM-based morphological analysis of fracture surfaces

Scanning electron microscopy (SEM) was performed on the fracture surfaces of 3D-printed samples at 100% infill density tested under tensile loading in order to qualitatively support the interpretation of the fracture mechanisms associated with the different printing orientations (0°, 45°, and 90°). Specimens printed at lower infill densities were not selected for SEM observation because their fracture surfaces are dominated by the intentionally generated macroscopic voids and open

internal architecture associated with the infill pattern, which would mainly reflect the designed geometry rather than local fracture mechanisms. Fig. 11 illustrates these observations, with an image of PLA-CB sample printed at 0°, revealing a morphology characterized by a clearly visible layered structure, corresponding to layers parallel to the direction of tensile force, as observed at a magnification of x78. The observations show relatively irregular surfaces with the notable presence of cavities and discontinuities between filaments, as indicated by the arrows.
These imperfections reflect poor interlayer adhesion as well as a heterogeneous distribution of material, favoring the initiation and propagation of cracks. Failure appears to be localized primarily at the interfaces between filaments, indicating that mechanical behavior is strongly governed by the interlayer bond quality rather than by the material's intrinsic strength. This morphology is consistent with the observed mechanical performance, particularly the limitation of strength due to the presence of internal weak zones, which has been reported in some previous studies [33].

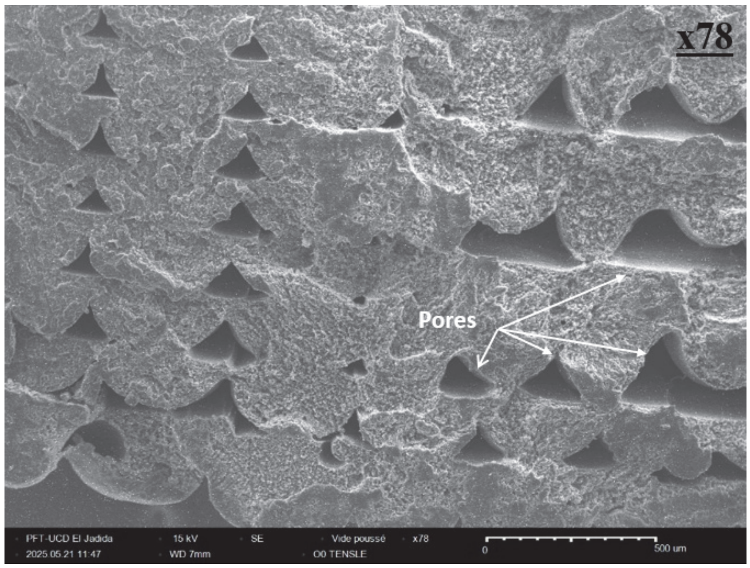

Figure 11: SEM image of the fracture surface of PLA-CB printed at 0° orientation (x78).

In contrast, the 45° printing direction results in a significantly stronger fracture response. The resulting fracture surfaces are noticeably more uniform and densely packed, indicating substantially better interlayer adhesion. Fig. 12 confirms this: the interfaces between adjacent filaments appear tighter and more continuous, suggesting that the strands fused more effectively during deposition. Rather than propagating along a single cleavage plane, the crack tends to track the inclined layer boundaries, producing a hybrid failure mechanism that combines tensile opening with shear sliding. We also observe more extensive plastic deformation near the fracture zone, confirming that this orientation allows the material to absorb considerably more energy before final rupture.

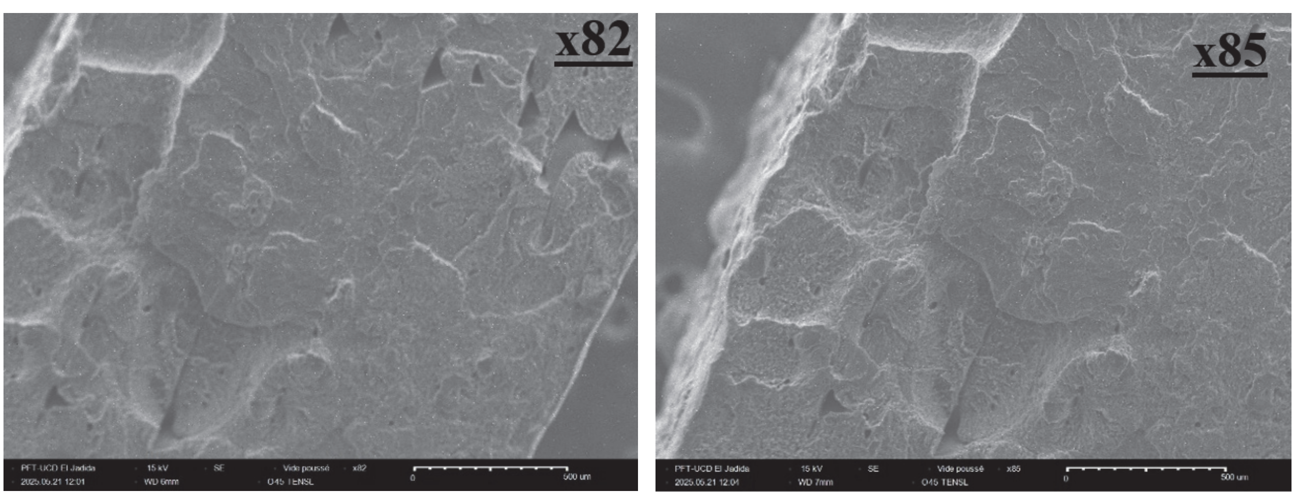

Figure 12: SEM image of the fracture surface of PLA-CB printed at 45° orientation (x82 and x85).

For the 90° orientation, with layers perpendicular to the direction of tensile stress, the fracture surface appears more heterogeneous, characterized by interlayer separations, small pores, and locally dense regions as observed in Fig. 13. In this configuration, fracture is primarily controlled by weak interlayer adhesion, leading to brittle behavior and rapid crack propagation along the interfaces. Overall, these observations highlight the decisive influence of the printing orientation on fracture mechanisms and confirm the direct relationship between the microstructure and the mechanical performance of PLA-CB composites.

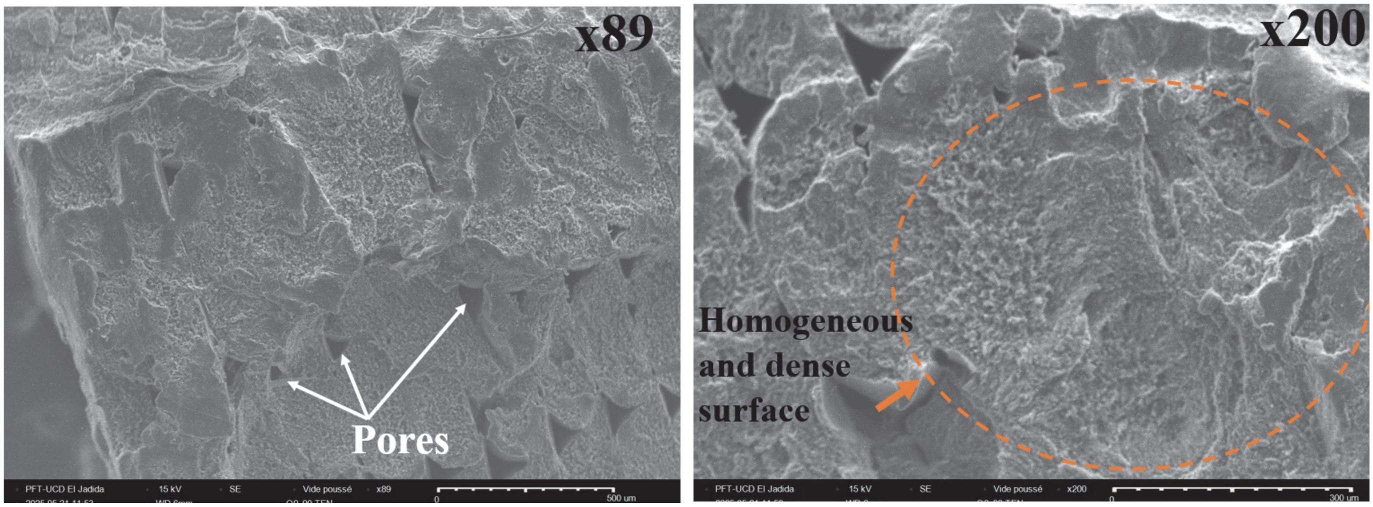

Figure 13: SEM image of the fracture surface of PLA-CB printed at 90° orientation (x89 and x200).

Reliability analysis of 3D-printed samples from tensile tests

The mechanical tests carried out clearly demonstrated and confirmed that the infill density and layer orientation directly influence how stresses are distributed, transmitted, and absorbed within the structure of the 3D-printed PLA-CB composite. In addition to these printing parameters, the final mechanical response may also be affected by local features generated during the FDM process, such as small voids, bead discontinuities, dimensional variations, and imperfect bonding between adjacent filaments. These factors can contribute to local stress concentration and may partly explain the dispersion observed in the tensile results.

Infill density is considered as a parameter that measures the distance between the lines of the internal infill of the printed part and, consequently, the percentage of solidity within the part. The results presented from tensile tests on PLA-CB showed a significant impact on mechanical properties depending on the internal infill of the parts. Samples with a density of 100% present the highest values in terms of stress and modulus of elasticity, thanks to a more compact structure and better continuity of the load path. However, the presence of voids in lower-density samples results in an unbalanced stress distribution, leading to premature failure. This effect may be amplified by local printing non-uniformities, especially at low infill densities, where the real internal morphology of the specimen can strongly influence the effective load-bearing area.

However, layer orientation remains the most significant factor in mechanical behavior. According to the results for PLA-CB as a conductive composite material, 0° orientation (parallel to the direction of the tensile force) offered the best mechanical performance. At 45°, the results show intermediate behavior between stiffness and flexibility due to the distribution of shear stress between the layers. In contrast, parts printed at 90° exhibit much lower strength, dominated by delamination between the layers. Thus, the observed tensile behavior can be understood as the result of both the selected printing parameters and the local morphology produced during the printing process.

For residual ultimate stress and strain

The Weibull probabilistic analysis of ultimate tensile strength (σu) for specimens printed in various orientations (0°, 45°, and 90°) is illustrated by the linear regression curves shown in Fig. 14. The remarkable linearity observed for all orientations ($R^2 > 0.94$) confirms that the failure behavior of the PLA-CB composite follows the two-parameter Weibull distribution. The Graphs in Fig. 14 show the slopes of each regression corresponds to the shape parameter (m), which represent the variability of the strength data: a higher shape parameter indicates more homogeneous material behavior and low data dispersion.

Although the samples printed with a 0° orientation exhibit the highest tensile strength value of 49.680 MPa, which indicates a higher load-bearing capacity, for the 45° orientation proves the highest Weibull modulus (m), at 44.127, reflecting improved reliability and reduced variability in the strength distribution. This apparent discrepancy highlights the difference between average performance and statistical consistency. At 0° orientation, the polymer chains and carbon black particles are closely aligned in the direction of the load, leading to increased strength, but also to greater sensitivity to local defects or bonding imperfections between layers,, which increases data dispersion.

Conversely, the 45° orientation leads to a uniform fracture pattern with lower absolute strength as the load is distributed in the inclined directions of the filaments. The 45° samples fracture more predictable and thus have a higher (m) value. The 90° orientation has the lowest form factor (16.595), suggesting that the strength values are slightly more dispersed. the scale parameter (η) refers to the characteristic strength at the point where 63.2% Of samples are susceptible to failure. As illustrated in Tab. 7, the 0° orientation exhibits the highest η value (49.77 MPa), that confirm its tensile strength is superior to that of the 90° and 45° orientations.

This suggests the strong alignment of the polymer chains and conductive particles along the direction of loading, which improves the charge transfer and the interlayer adhesion. On the other hand, the lower values of η obtained for the 90° and 45° orientations indicate a lower mechanical strength due to a weaker interlayer bonding or a load redistribution along the inclined paths of the filaments. Consequently, although the 45° specimens exhibit the highest Weibull modulus, indicating lower dispersion and more predictable failure behavior, the 0° orientation remains the strongest configuration in terms of characteristic tensile strength and critical stress.

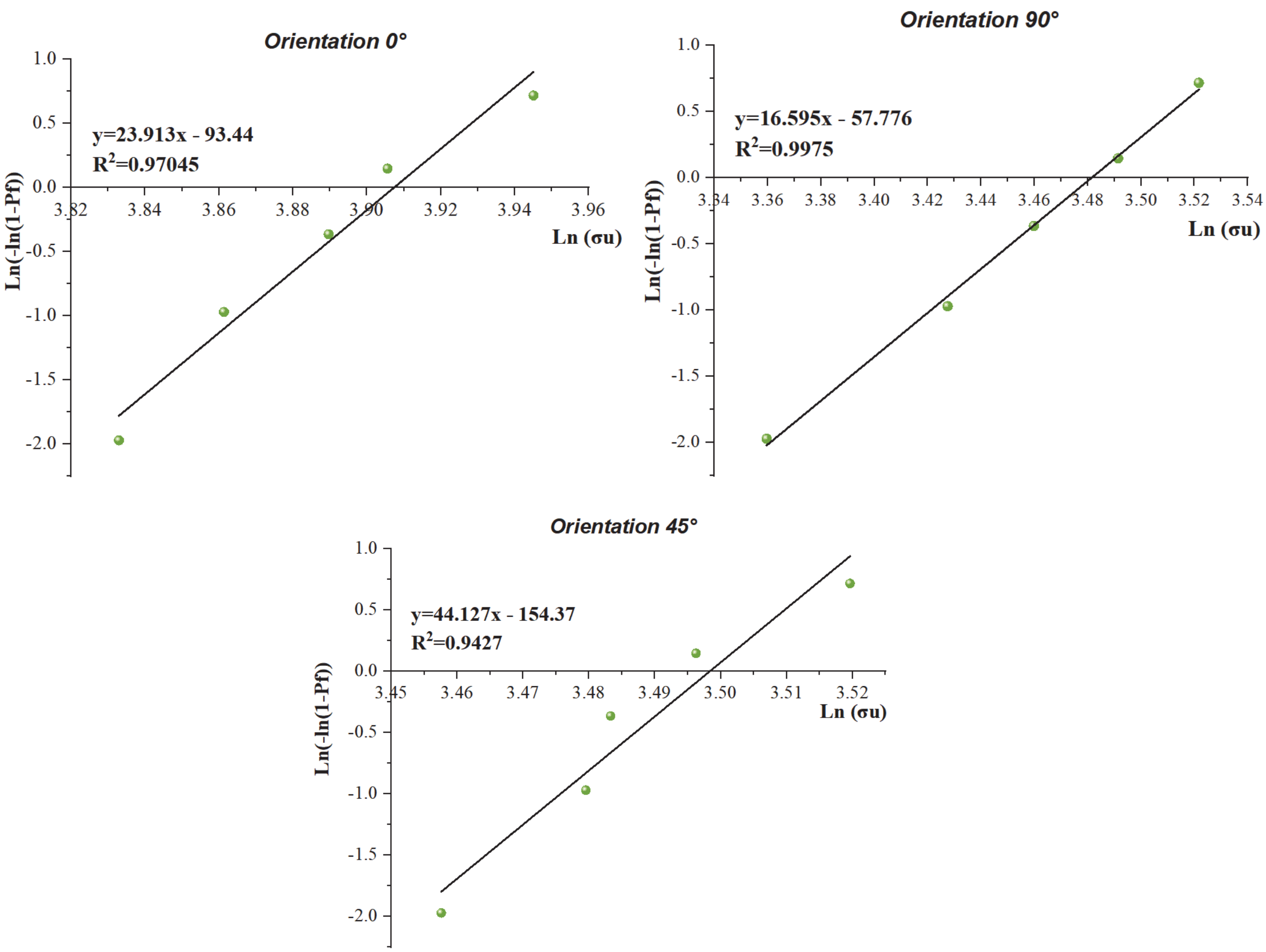

Figure 14: Linear regression analysis of experimental tensile stress data of PLA-CB under tensile test as a function of layer orientation: 0°, 90° and 45°.

Weibull parameters (Ultimate Stress data)	Equation	Shape factor, m	Scale factor; η (MPa)
Orientation 0°	Y=23.913x – 93.44	23.913	49.774
Orientation 90°	Y=16.595x – 57.776	16.595	32.509
Orientation 45°	Y=44.127x – 154.37	44.127	33.059

Table 7: Experimental values of Weibull parameters for tensile stress under the influence of layer orientation.

Weibull linearization for the ultimate strain εu at failure also show good linearity for all orientations studied (R^2 ≈0.85 to 0.97), confirming that the strain at failure of PLA-CB is also well described by a two-parameter Weibull model. The clear trend of the curves in Fig. 15 represents the highest value (m) of ≈33.034 for the 45° orientation, which indicates the least dispersion and hence the most predictable strain at failure. In contrast, the values of the shape factor for the 0° and 90° orientations are significantly lower, at about ≈9.50 and 9.44, respectively, which reflects a higher level of variation of the individual samples. From a mechanical point of view, the 45° orientation induces a combination of tension and shear in several filament paths. The micropores are more uniformly developed and a more uniform deformation at failure is observed. In the case of 0° and 90° orientation, the deformation is dominated by the interlayer bonding in some planes. The local porosity, filament misalignment or bonding defects can induce a higher variability in εu. Tab. 8 also shows the values of the scale parameter η. This value is slightly higher for 0° than for 90°, and both are higher than for the 45° orientation, indicating that the 0° and 90° specimens, on average, withstand the greatest strain before failure, while those at 45° fail at a slightly lower characteristic strain, but in a very consistent manner. This reflects the trade-off already observed in the stress-based Weibull results.

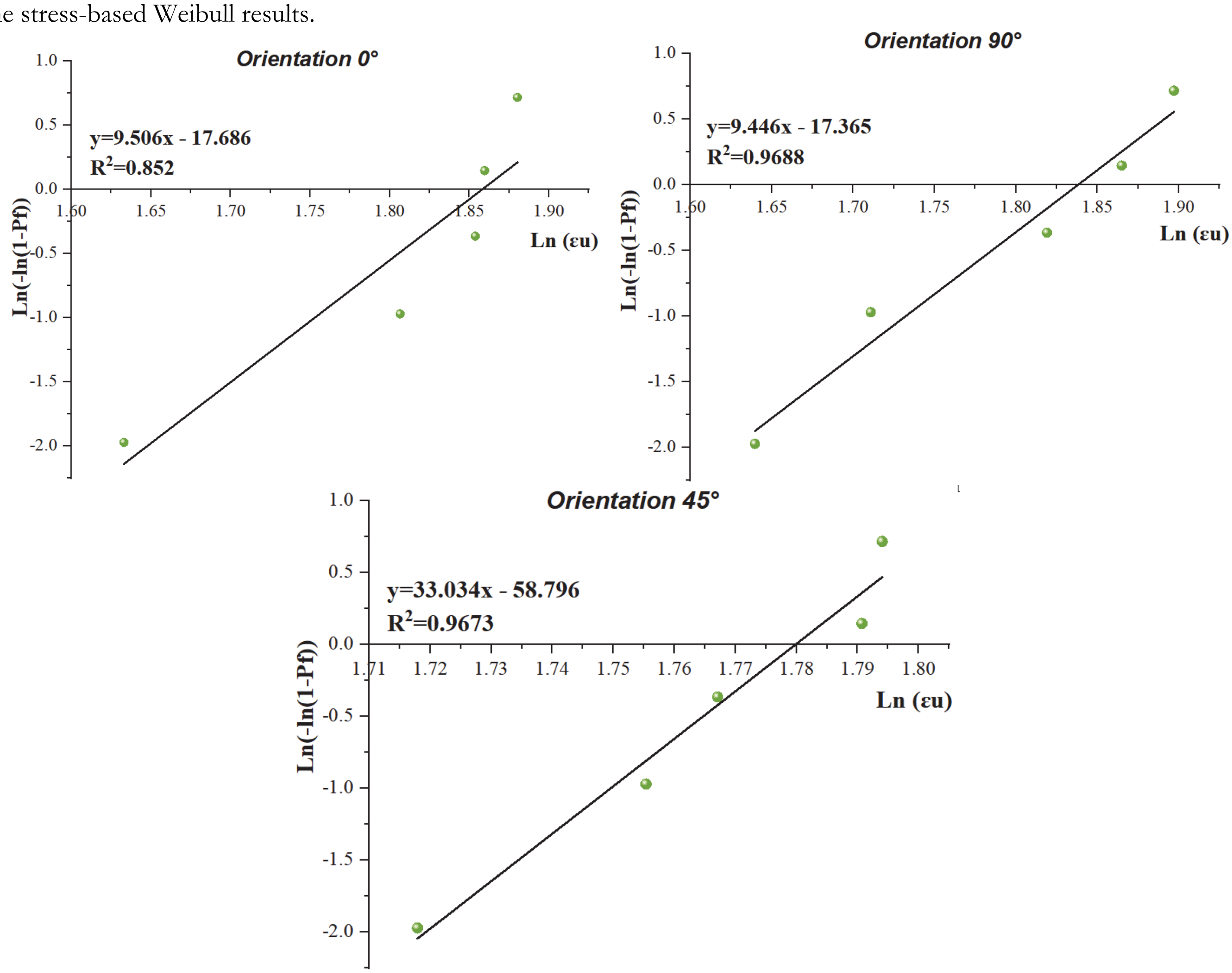

Figure 15: Linear regression analysis of ultimate strain at failure data of PLA-CB under tensile test as a function of layer orientation: 0°, 90° and 45°.

Weibull parameters (Strain at failure data)	Equation	Shape factor, m	Scale factor, η (MPa)
Orientation 0°	Y=9.506x – 17.44	9.506	6.426
Orientation 90°	Y=9.446x – 17.365	9.446	6.285
Orientation 45°	Y=33.034x – 58.796	33.034	5.929

Table 8: Experimental values of Weibull parameters for ultimate strain at failure under the influence of layer orientation.

The graphs of the Ps-Pf in Fig. 16 show that the probability of survival and failure of the PLA-CB composite in the three printing orientations varies with increasing applied stress. The two curves cross at the critical stress σc, which is the typical stress level at which half of the tested samples are expected to fail. The intersection occurs at around 49.01 MPa for the 0° orientation, which shows the best tensile strength, as the printed filaments are oriented in the direction of the load, providing effective stress transfer through the material.
On the other hand, 45° and 90° orientations showed less critical stresses, which are about 32.78 MPa, and 31.79 MPa, respectively. The 45° curve shows a more pronounced transition between Ps and Pf, indicating a narrower stress distribution and more predictable fracture behavior, which corresponds to its higher Weibull modulus (m). Conversely, the 90° orientation exhibits a gentler crossover, reflecting greater data dispersion and lower reliability, most likely caused by weaker interlayer bonding when the filaments are oriented perpendicular to the tensile axis.

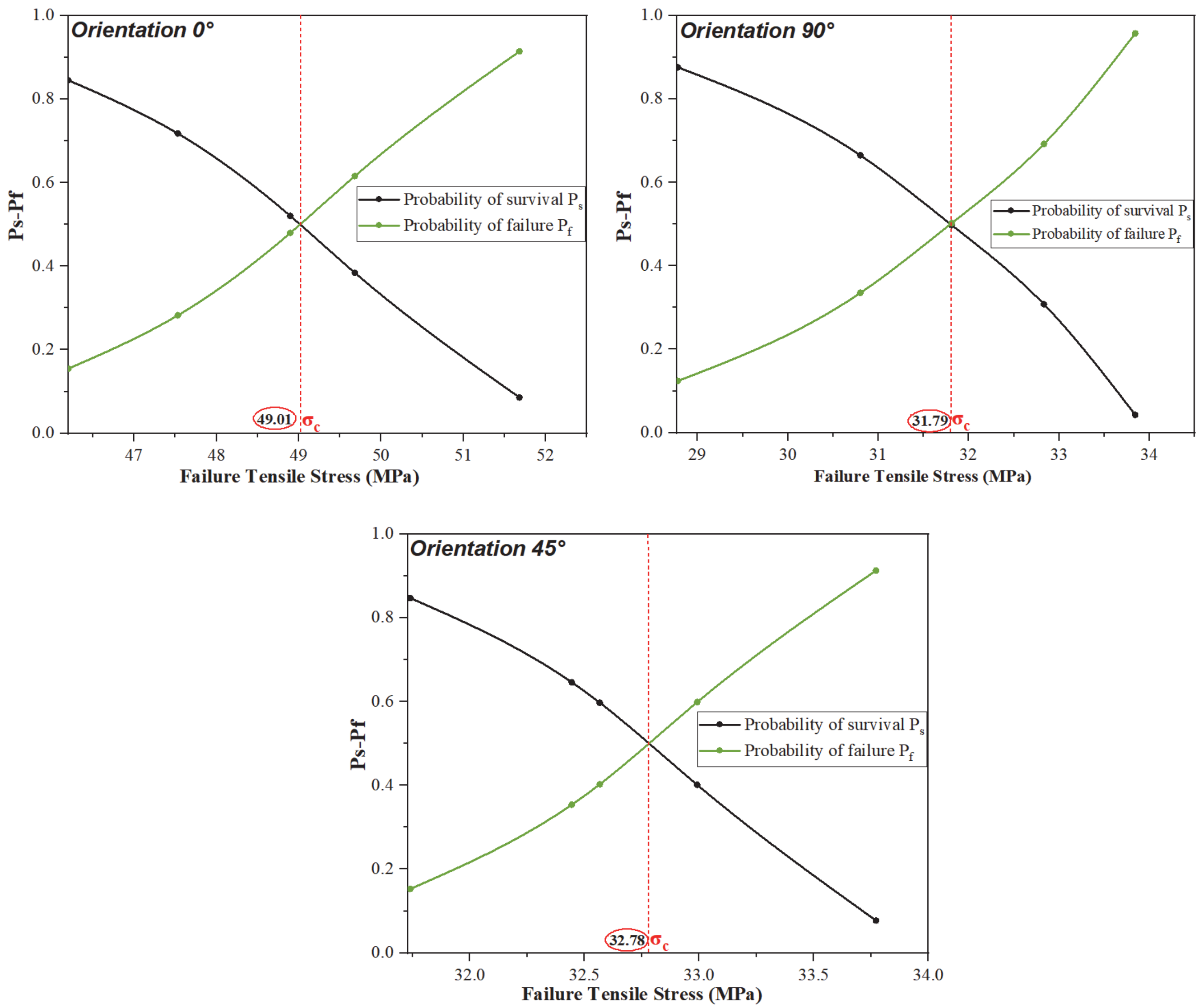

Figure 16: Evolution of Ps-Pf curves of tensile Strength for PLA-CB under the influence of layer orientation 0°, 90° and 45°.

The Ps-Pf curves based on the strain at failure (ε) are displayed in Fig. 17. The probability of failure (Pf), which represents the statistical accumulation of damage within the specimen, rises as the material experiences increased strain. In the meantime, the probability of survival (Ps) progressively decreases. This opposite trend only verifies that (Ps) continuously decreases as the material deforms more and gets closer to failure. The intersection of the two curves represents the critical strain (εc), which is the characteristic strain at which 50% of the specimens are likely to fail.
The critical strain for the 0° orientation is close to 6.18%, suggesting that samples printed in the direction of the load may withstand the most strain before failing. Effective elongation and energy dissipation are made possible by the alignment of conductive particles and polymer chains with the tensile axis. With a slightly lower εc value of 6.04%, the 45° orientation appears to have a more constrained deformation capacity. On the other hand, because of poorer interlayer adhesion and an earlier beginning of delamination, the 90° orientation exhibits the lowest εc value of 5.86%.

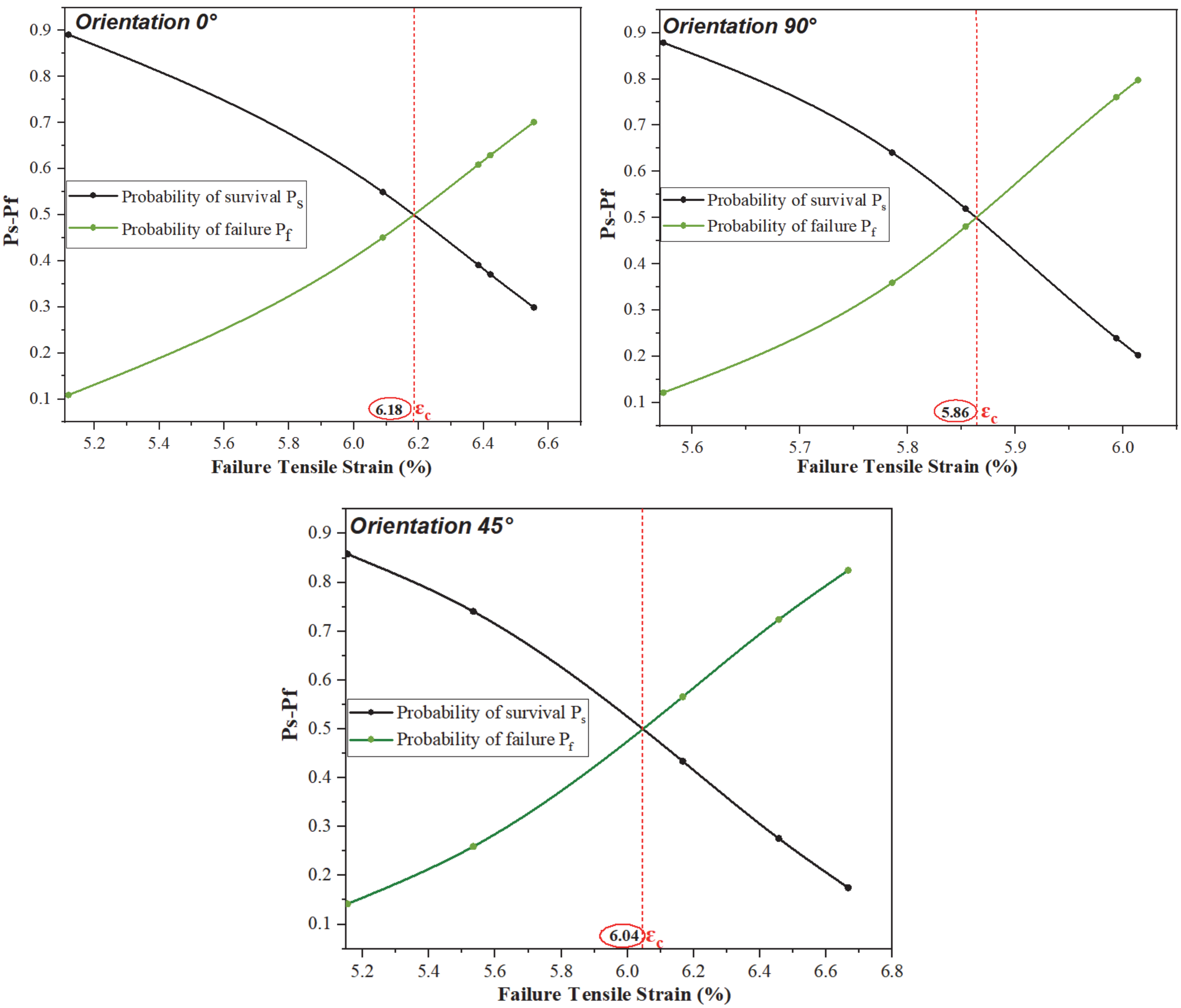

Figure 17: Evolution of Ps-Pf curves of Tensile Strain at failure for PLA-CB under the influence of layer orientation 0°, 90° and 45°.

Fig. 18 shows a comparative analysis of the experimental critical stress (σc) and critical strain (εc) obtained for different printing orientations of the PLA-CB composite. A clear influence of the mechanical parameters depending on the sample configuration can be observed.
However, the 0° configuration exhibits the highest σc value (49.01 MPa) and the most significant εc value (6.18%), confirming that the alignment of the filaments along the tensile axis maximizes both strength and elongation. The 90°

orientation exhibits moderate strength (31.78 MPa) and slightly lower elongation (6.04%), which corresponds to delamination between layers under tension. The 45° orientation, respectively, shows intermediate results (σc = 32.77 MPa and εc = 5.86%): lower strength than the 0° orientation, but stable and predicted deformation behavior due to mixed load paths along the filament directions.

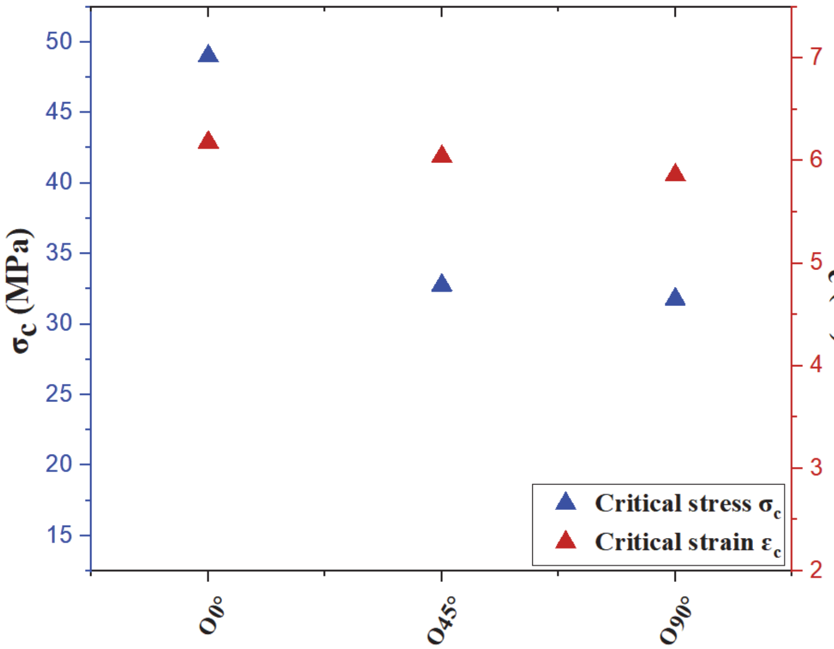

Figure 18: Comparative graph of the critical stress (σc) and critical strain (εc) for different layer orientations.

For residual lifetime

The higher Weibull modulus obtained for the 45° orientation in the ultimate stress and strain analyses reflects lower data dispersion and a more predictable failure behavior, rather than a higher residual lifetime reliability. In the residual lifetime analysis, reliability and damage are evaluated as a function of the life fraction. Under this approach, the 0° orientation remains the most favorable configuration, showing the slowest damage accumulation and the latest transition toward accelerated degradation. The 45° orientation therefore shows an intermediate response: although its failure behavior is statistically more consistent, its inclined filament arrangement promotes tensile-shear damage earlier than in the 0° orientation.

Fig. 19 illustrates the trend in cumulative damage (Ds) and reliability (R) as a function of remaining lifetime (β) for the three printing angles examined: 0°, 45°, and 90°. In this study, the life fraction β was considered as a dimensionless normalized indicator describing the progression of damage within the Weibull-based reliability framework. The curves for each angle follow the Weibull model. This means that damage and reliability are directly proportional but tend in opposite directions: as damage increases, reliability decreases. The critical threshold βc corresponds to the transition region where damage accumulation becomes more pronounced and the reliability curve starts to decrease more rapidly. Therefore, β and βc were used to compare the relative damage sensitivity of the different printing orientations under the investigated tensile conditions. This approach allows us to track the rate of damage propagation and estimate the influence of the printing direction on the relative residual-life performance of the PLA-CB specimens to be evaluated.

The results clearly indicate that FDM printing induces anisotropic behaviour, mainly due to the way the layers are deposited. Printed specimen at 0° orientation exhibits the lowest damage accumulation rate and the highest reliability among the three orientations (0°, 45°, 90°). This behaviour indicates that an increased interlayer cohesion and filament alignment parallel to the loading direction allow for a more efficient stress transmission and an improved resistance to the applied stress. The critical lifetime fraction is also about the βc0° = 45%, which indicates the transition to the damage acceleration stage takes place relatively late, thus implying a delayed degradation process and a better structural stability. On the other hand, specimens printed at 45° show an intermediate behaviour. The reliability falls faster and the damage accumulation starts earlier at the critical lifetime fraction of about βc45°=35%. The observed behaviour can be attributed to the inclined filament arrangement which leads to a combined tensile-shear loading regime at the interlayer interfaces. This distribution of stresses promotes the early formation of microcracks and weakens the interface zones, which contributes to

a faster degradation rate and a shorter service life than the 0° orientation. However, for the 90° orientation, when the load is applied perpendicular to the deposited layers, the reliability decreases significantly and damage increases almost immediately, with a much lower value of approximately βc90° ≈ 29%. This behavior indicates that delamination between the layers predominates and that failure occurs after a shorter residual life due to the low adhesion between the layers.
The general trend follows a decreasing order of reliability and service life as follows: 0° > 45° > 90°. The increasing gap between reliability R(t) and static damage Ds(t) for the highest angles confirms that the rate of damage propagation accelerates when the material is subjected to a transversely directed load relative to the printing direction.

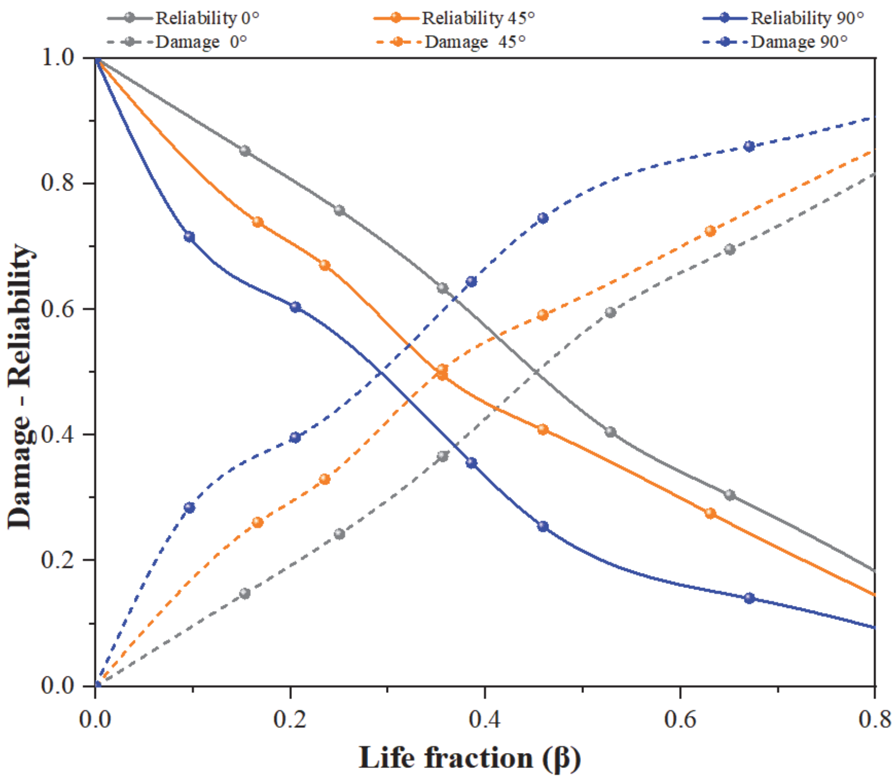

Figure 19: Evolution of Weibull static damage and reliability as a function of the life fraction (β) under the influence of layer orientation.

CONCLUSION

This experimental study focuses on a deterministic and probabilistic approach to estimate the experimental damage of the PLA-CB composite material under tensile loading. Key characteristics, such as strength, strain at break, and residual lifetime are determined as a function of layer orientation in 3D-printed PLA-CB. The Weibull analysis presented in this study is used to determine probabilistic values which represent the critical load level requiring intervention. This is when the material reaches the stage of accelerated damage, where deformation exceeds the material's tolerable limits, reaching the plastic and brittle thresholds, ultimately leading to fracture. The results show that layer orientation significantly affect the material's mechanical performance. Specifically, higher tensile orientation influence stress concentration and fracture mechanisms.

NOMENCLATURE

3D : Three-Dimensional
PLA : Polylactic Acid
CB : Carbon Black
FDM : Fused Deposition Modelling
CAD: Computer-Aided Design

STL: Stereolithography file format
SLA: Stereolithography
SLS: Selective Laser Sintering
FFF: Fused Filament Fabrication
SEM : Scanning Electron Microscopy
σ_u : Ultimate tensile strength
m : Weibull shape factor
η : Weibull scale factor
ε_u : ultimate strain
Ps : Probability of survival
Pf : Probability of failure
σc : Critical Stress
εc : Critical Strain
β : Life fraction
β_c : Critical life fraction
R: Reliability

REFERENCES

[1] Starkova, O., Gagani, A. I., Karl, C. W., Rocha, I. B. C. M., Burlakovs, J., and Krauklis, A. E., (2022). Modelling of Environmental Ageing of Polymers and Polymer Composites—Durability Prediction Methods, Polymers, 14(5), DOI: https://doi.org/10.3390/polym14050907.

[2] Taoufik, H., Fatima, M., and Hassan, R. (2023). Modeling of the Fracture Behavior of the 3D Printed Polymers Using XFEM, Procedia Structural Integrity, 47, pp. 711–722. DOI: https://doi.org/10.1016/j.prostr.2023.07.048.

[3] Djeghader, D., and Redjel, B. (2024). Evaluation of Fatigue Life of Fiberglass Reinforced Polyester Composite Materials Using Weibull Analysis Methods, Composites and Advanced Materials, 33. DOI: https://doi.org/10.1177/26349833241239800.

[4] Sindhu, T. N., Shafiq, A., Lone, S. A., Al-Mdallal, Q. M., and Abushal, T. A. (2024). Distributional Properties of the Entropy Transformed Weibull Distribution and Applications to Various Scientific Fields, Scientific Reports, 14(1). DOI: https://doi.org/10.1038/s41598-024-83132-w.

[5] D'andrea, D., Risitano, G., Raffaele, M., Cucinotta, F., and Santonocito, D. (2022). Damage Assessment of Different FDM-Processed Materials Adopting Infrared Thermography, Frattura ed Integrita Strutturale, 16(62), 2022, pp. 75–90. DOI: https://doi.org/10.3221/IGF-ESIS.62.06.

[6] Tabatabaee, S. M. J., and Fakoor, M. (2023). Investigation into Effective Mechanical Properties of Porous Material Produced by the Additive Manufacturing Method, Frattura ed Integrita Strutturale, 17(65), pp. 208–223. DOI: https://doi.org/10.3221/IGF-ESIS.65.14.

[7] Taoufik, H., Fouad, A. H., and Fatima, M. (2025). Damage of Additively Manufactured Polymer Materials: Experimental and Probabilistic Analysis," Fracture and Structural Integrity, 19(73), pp. 236–255. DOI: https://doi.org/10.3221/IGF-ESIS.73.16.

[8] Hachimi, T., Ait Hmazi, F., Arhouni, F. E., Rejdali, H., Riyad, Y., and Majid, F., "Experimental Calibration of a Virtual Raster Section for High-Accuracy FDM Simulation in Abaqus," Fracture and Structural Integrity, Vol. 20, No. 76, 2026, pp. 31–48. https://doi.org/10.3221/igf-esis.76.03.

[9] Naboulsi, N., Majid, F., Hachimi, T., Dadoun, S., Barhoumi, N., and Khlifi, K. (2025). Predicting the Strength of 3D-Printed Conductive Composite under Tensile Load: A Probabilistic Modeling and Experimental Study, Fracture and Structural Integrity, 19(72), pp. 247–262. DOI: https://doi.org/10.3221/IGF-ESIS.72.18.

[10] Les, J. P., and Mat, D. (2006). Le Modèle de Weibull : Un Critère de Rupture Probabiliste, 1, pp. 1–9.

[11] Linardi, D., Monaldo, E., and Marfia, S. (2026). Evaluating the Role of Printing Orientation and Infill Strategy on 3D-Printed PLA Failure Mechanisms, Engineering Failure Analysis, 186, 110487. DOI: https://doi.org/10.1016/j.engfailanal.2025.110487.

[12] Adarsh, S. H., and Nagamadhu, M. (2025). Effect of Printing Parameters on Mechanical Properties and Warpage of 3D-Printed PEEK/CF-PEEK Composites Using Multi-Objective Optimization Technique, Journal of Composites Science, 9(5). DOI: https://doi.org/10.3390/jcs9050208.

[13] Akçay, Ö., and Arı, A. (2025). Effect of Infill Density and Infill Pattern on Mechanical Properties of 3D-Printed PLA Produced by FFF, Fırat Üniversitesi Mühendislik Bilimleri Dergisi, 37(1), pp. 223–232. DOI: https://doi.org/10.35234/fumbd.1538296.
[14] Amirian, A., Battley, M., Diegel, O., and Amirpour, M. (2025). Additive Manufacturing Defects in Polymeric Lattice Structures: A Comprehensive Analysis of Morphology, Distribution, and Printing Orientation Influence, International Journal of Advanced Manufacturing Technology, 140(9–10), pp. 5361–5384. DOI: https://doi.org/10.1007/s00170-025-16521-8.
[15] Qamar Tanveer, M., Mishra, G., Mishra, S., and Sharma, R. (2022). Effect of Infill Pattern and Infill Density on Mechanical Behaviour of FDM 3D Printed Parts- a Current Review, Materials Today: Proceedings, 62 pp. 100–108. DOI: https://doi.org/10.1016/j.matpr.2022.02.310.
[16] Brackett, J., Cauthen, D., Condon, J., Smith, T., Gallego, N., Kunc, V., and Duty, C. (2022). The Impact of Infill Percentage and Layer Height in Small-Scale Material Extrusion on Porosity and Tensile Properties, Additive Manufacturing, 58, p. 103063. DOI: https://doi.org/10.1016/J.ADDMA.2022.103063.
[17] Parodo, G., Sorrentino, L., Turchetta, S., and Moffa, G. (2025). Evaluation of the Accuracy of a Fused Deposition Modeling Process in the Production of Low-Density ABS Lattice Structures, Materials, 18(7), pp. 1–17. DOI: https://doi.org/10.3390/ma18071679.
[18] Naboulsi, N., Majid, F., and Louzazni, M. (2025). Environmentally Friendly PLA-Based Conductive Composites : Electrical and Mechanical Performance, pp. 1–23.
[19] Glogowsky, A., Korger, M., and Rabe, M. (2024). Influence of Print Settings on Conductivity of 3D Printed Elastomers with Carbon-Based Fillers, Progress in Additive Manufacturing, 9(4), pp. 791–803. DOI: https://doi.org/10.1007/s40964-023-00483-y.
[20] Marion, S., Joffre, T., Jaxel, J., and Pigeonneau, F. (2023). Improved Printability and Electrical Conductivity of Carbon Black Polymer Composite with a Customized Nozzle of Material Extrusion Process, Additive Manufacturing, 79. DOI: https://doi.org/10.1016/j.addma.2023.103939.
[21] Naboulsi, N., Majid, F., Hmazi, F. A., Baghaz, E., El Alaoui-Belghiti, H., and Kechagias, J. D. (2025). Electrical Conductivity and Microstructural Features of 3D-Printed PLA-CB Composites Fabricated at Different Temperatures, Next Materials, 9. https://doi.org/10.1016/j.nxmate.2025.101122.
[22] Cheng, Y., Wang, J., Shao, M., Liang, Y., and Li, H. (2025). Hybrid Combinations of Graphene Nanoplatelet, Carbon Nanotube, and Carbon Black for Tailored Mechanical and Triboelectric Properties in Polypropylene Fibers, Advanced Composites and Hybrid Materials, 8(3). DOI: https://doi.org/10.1007/s42114-025-01341-x.
[23] Yang, J., Liu, H., Cai, G., and Jin, H. (2025). Additive Manufacturing and Influencing Factors of Lattice Structures: A Review, Materials, 18(7). DOI: https://doi.org/10.3390/ma18071397.
[24] Varsavas, S. D., Michalec, P., and Arbeiter, F. (2025). A Comprehensive Study on Thermoplastic Elastomers for Additive Manufacturing of Leg Prosthesis, Next Materials, 8. DOI: https://doi.org/10.1016/j.nxmate.2025.100700.
[25] Wickramasinghe, S., Do, T., and Tran, P. (2020). FDM-Based 3D Printing of Polymer and Associated Composite: A Review on Mechanical Properties, Defects and Treatments, Polymers, 12(7), pp. 1–42. DOI: https://doi.org/10.3390/polym12071529.
[26] Mwema, F. M., and Akinlabi, E. T. (2020). Basics of Fused Deposition Modelling (FDM), SpringerBriefs in Applied Sciences and Technology, pp. 1–15. DOI: https://doi.org/10.1007/978-3-030-48259-6_1.
[27] Luo, Y., Xiong, S. Y., Zhang, F., He, X. X., Lu, X., and Peng, R. T. (2021). Preparation of Conductive Polylactic Acid/High Density Polyethylene/Carbon Black Composites with Low Percolation Threshold by Locating the Carbon Black at the Interface of Co-Continuous Blends, Journal of Applied Polymer Science, 138(17), 2021, pp. 1–11. DOI: https://doi.org/10.1002/app.50291.
[28] Zhao, H., Liu, X., Zhao, W., Wang, G., and Liu, B. (2019). An Overview of Research on FDM 3D Printing Process of Continuous Fiber Reinforced Composites, Journal of Physics: Conference Series, 1213(5). DOI: tps://doi.org/10.1088/1742-6596/1213/5/052037.
[29] Hachimi, T., Naboulsi, N., Majid, F., Rhanim, R., Mrani, I., and Rhanim, H. (2021). Design and Manufacturing of a 3D Printer Filaments Extruder, Procedia Structural Integrity, 33, pp. 907–916. DOI: https://doi.org/10.1016/j.prostr.2021.10.101.
[30] Naboulsi, N., Hachimi, T., Majid, F., Rhanim, R., Zekriti, N., and Rhanim, H., (2021). Modeling and Control of 3D Filament Extruder," Procedia Structural Integrity, 33, pp. 989–995. DOI: https://doi.org/10.1016/j.prostr.2021.10.109
[31] Delia, S., Rochman, A., and Curmi, A. (2024). Factors Affecting Interface Bonding in Multi-Material Additive Manufacturing, Progress in Additive Manufacturing, 9(5), pp. 1365–1379. DOI: https://doi.org/10.1007/s40964-024-00617-w.

[32] Thirugnanasambandam, A., Packkirisamy, V., Narayanaswamy, N., Rangappa, S. M., Siengchin, S., and Kechagias, J. D. (2025). Influence of Infill Patterns on the Mechanical and Antibacterial Properties of 3D-Printed Polylactic Acid Reinforced with Hydroxyapatite/Magnesium Oxide Bone Repair Scaffolds, Emergent Materials, DOI: https://doi.org/10.1007/s42247-025-01141-5.
[33] Islam, M. S., Elahee, G. M. F., Fang, Y., Yu, X. (Bill), Advincula, R. C., and Cao, C. (2025). Polylactic Acid (PLA)-Based Multifunctional and Biodegradable Nanocomposites and Their Applications, Composites Part B: Engineering, 306,. DOI: https://doi.org/10.1016/j.compositesb.2025.112842.